Journal of Atmospheric and Solar-Terrestrial Physics 123 (2015) 102–112

Contents lists available at ScienceDirect

Journal of Atmospheric and Solar-Terrestrial Physics

journal homepage: www.elsevier.com/locate/jastp

Solar flares induced D-region ionospheric and geomagnetic perturbations

R. Selvakumaran[a], Ajeet K. Maurya[b], Sneha A. Gokani[a], B. Veenadhari[a], Sushil Kumar[c], K. Venkatesham[b], D.V. Phanikumar[d], Abhay K. Singh[e], Devendraa Siingh[f], Rajesh Singh[b,*]

[a] Indian Institute of Geomagnetism, Kalamboli Highway, New Panvel, Navi Mumbai 410218, Maharashtra, India
[b] KSK Geomagnetic Research Laboratory, Hanumanganj, Allahabad 221505, India
[c] School of Engineering and Physics, The University of South Pacific, Suva, Fiji
[d] Aryabhatta Research Institute of Observational Sciences, Nainital, India
[e] Atmospheric Research Laboratory, Department of Physics, Banaras Hindu University, Varanasi 221005, India
[f] Indian Institute of Tropical Meteorology, Pune, India

ARTICLE INFO

Article history:
Received 13 June 2014
Received in revised form
11 December 2014
Accepted 23 December 2014
Available online 26 December 2014

Keywords:
Solar flares
VLF (very low frequency) waves
D-region ionosphere

ABSTRACT

The D-region ionospheric perturbations caused by solar flares which occurred during January 2010–February 2011, a low solar activity period of current solar cycle 24, have been examined on NWC transmitter signal (19.8 kHz) recorded at an Indian low latitude station, Allahabad (Geographic lat. 25.75°N, long. 81.85°E). A total of 41 solar flares, including 21 C-class, 19 M-class and 01 X-class, occurred during the daylight part of the NWC-Allahabad transmitter receiver great circle path. The local time dependence of solar flare effects on the change in the VLF amplitude, time delay between VLF peak amplitude and X-ray flux peak have been studied during morning, noon and evening periods of local daytime. Using the Long Wave Propagation Capability code V 2.1 the D-region reference height (H') and sharpness factor (β) for each class of solar flare (C, M and X) have been estimated. It is found that D-region ionospheric parameters (H', β) strongly depend on the local time of flare's occurrence and their classes. The flare time electron density estimated by using H' and β shows maximum increase in the electron density of the order of ~80 times as compared to the normal day values. The electron density was found to increase exponentially with increase in the solar flux intensity. The solar flare effect on horizontal component (H) of the Earth's magnetic field over an equatorial station, Tirunelveli (Geographic lat., 8.7°N, long., 77.8°E, dip lat., 0.4°N), shows a maximum increase in H of ~8.5% for M class solar flares. The increase in H is due to the additional magnetic field produced by the ionospheric electrojet over the equatorial station.

1. Introduction

Solar flares are known to cause perturbations in the daytime ionosphere (*e.g.,*Mitra, 1974; Davies, 1990; Tsurutani et al., 2009) but it is the D-region of the ionosphere which is perturbed the most (Mitra, 1974; Zigman et al., 2007). During the daytime, the D-region ionization is maintained mainly by direct Lyman-α (121.6 nm) radiation from the Sun which partially ionizes the nitric oxide (N_2O, at ~70 km altitude), a minor neutral constituent in the D-region. Under the normal conditions, the solar X-ray flux is too small to be a significant source of ionization but during solar flares the increased X-ray flux from the Sun in the wavelength range of 0.2–0.8 nm ionizes neutral constituents along with the major O_2 and N_2 species (Hargreaves, 2003; Mitra, 1974). This in turn modifies the electron density in the D-region ionosphere and hence changes the propagation conditions of Very Low Frequency (VLF, 3–30 kHz) waves in the Earth-ionosphere waveguide (EIWG) formed between the D-region ionosphere and the Earth's surface (Thomson et al., 2005).

The measurement of VLF signals, generated by navigational transmitters has emerged as one of the reliable tools for remote sensing of the D-region electron density perturbations associated with solar flares (Mitra, 1974; Ananthakrishnan et al., 1973; Thomson et al., 2004; Grubor et al., 2005; Kumar and Kumar, 2014; Maurya et al., 2014a,b). The D-region monitoring is rather difficult due to its altitude range, which is too high for balloons and too low

* Corresponding author. Fax: +91 532 2567030.
E-mail addresses: selva2986@gmail.com (R. Selvakumaran), ajeetphoton09@gmail.com (A.K. Maurya), gokanisneha@gmail.com (S.A. Gokani), veenaiig@gmail.com (B. Veenadhari), kumar_su@usp.ac.fj (S. Kumar), kvenkatesh.physics@gmail.com (K. Venkatesham), astrophani@gmail.com (D.V. Phanikumar), abhay_s@rediffmail.com (A.K. Singh), devendraasiingh@tropmet.res.in (D. Siingh), rajeshsing03@gmail.com (R. Singh).

http://dx.doi.org/10.1016/j.jastp.2014.12.009
1364-6826/

for satellite measurements. Rockets and Radars have been used, but they have poor spatial and temporal resolutions and hence cannot be used for continuous monitoring of the D-region ionosphere. The VLF remote sensing is also a cost-effective technique for understanding the dynamical processes in the D-region ionosphere (Bainbridge and Inan, 2003; Maurya et al., 2010; Phanikumar et al., 2014; Singh et al., 2011, 2012; Thomson et al., 2007; Thomson and McRae, 2009).

There have been several studies (*e.g.*,Ananthakrishnan et al., 1973; Pant, 1993; Thomson and Clilverd, 2001; McRae and Thomson, 2000, 2004; Thomson et al., 2005; Grubor et al., 2005; Zigman et al., 2007; Singh et al., 2013) on the D-region solar flare effects using VLF waves, transmitted by the navigational transmitters. Some studies mainly focused on the comparative investigations between the changes in the VLF signal amplitude/phase and time delay with respect to solar X-ray flux (Ananthakrishnan et al., 1973; Pant, 1993) however local time dependence of these perturbations was not considered. Several studies (*e.g.*, Thomson and Clilverd, 2001; McRae and Thomson, 2004; Thomson et al., 2005; Grubor et al., 2005, 2008; Zigman et al., 2007) on the D-region solar flare effects using Long Wave Propagation Capability (LWPC) code (developed by Naval Ocean Systems Center (NOSC), San Diego, USA) (Morfitt and Shellman, 1976), have estimated Wait ionospheric parameters; D-region reflection height (H') in km and D-region electron density gradient or sharpness factor (β) in km^{-1} (Wait and Spies, 1964). The quantification of the D-region reflection height and electron density changes during flare events had been reported by several researchers (Thomson and Clilverd, 2001; McRae and Thomson, 2004; Thomson et al., 2005; Zigman et al., 2007; Singh et al., 2013). The increased ionization due to a flare lowers the H' roughly in proportion to the logarithm of the X-ray flares intensity (McRae and Thomson, 2004).

The present study deals with the D-region ionospheric perturbations caused by solar flares during January 2010–February 2011 on NWC transmitter signal (19.8 kHz) recorded at an Indian low latitude station, Allahabad (Geographic lat. 25.40°N, long. 81.93°E). Solar flare effects on the horizontal component (H) of the Earth's magnetic field over an equatorial station, Tirunelveli (Geographic lat., 8.7°N, long., 77.8°E, dip lat., 0.4°N) have also been studied for the same period. The period of observations falls under the low solar activity period, beginning of the current solar cycle 24 after an extended solar minimum. The amplitude perturbations on NWC signal due to 41 solar flares (21 C-class, 19 M-Class and 1 X-class), have been analyzed. The local time variation of solar flare effects on the change in the VLF amplitude (ΔA), time delay (Δt) between the VLF peak amplitude and X-ray flux peak, changes in the horizontal component (ΔH) of the Earth's magnetic field, D-region reflection height (H') and sharpness factor (β), have been examined.

2. Experimental setup and data

The Automatic Weather Electromagnetic System for Observation Modeling and Education (AWESOME) VLF receiver located at Allahabad (Geographic lat. 25.40°N, long. 81.93°E; Geomagnetic lat., 16.25°N) is used to record the VLF signal (at 19.8 kHz) transmitted by NWC transmitter (Geographic lat. 21.80°S, long. 114.20°E), Australia. Further details of the VLF recording system at receiver sites in the Indian region can be found in the paper by Singh et al. (2010). The Transmitter Receiver Great Circle Path (TRGCP) from NWC transmitter to receiving station at Allahabad is shown in Fig. 1. TRGCP path length is about ~6400 km for NWC-Allahabad path, which falls under medium path length under the path classification given by Clilverd et al. (2001). The solar flares of

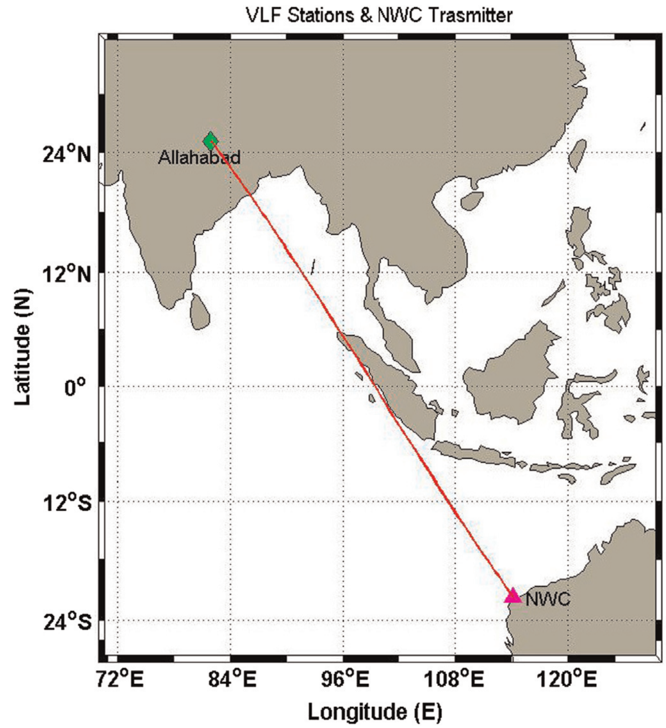

Fig. 1. Great Circle path between VLF transmitter NWC (pink triangle) and low latitude receiving stations in India Allahabad (green diamond).

C, M and X classes which occurred during January 2010 to February 2011 are selected for analysis depending upon the availability of VLF data at Allahabad. The Earth's geomagnetic field horizontal component (H) data (one second resolution) is obtained from equatorial station, Tirunelveli (Geographic lat. 8.7°N, long. 77.8°E, dip latitude: 0.4°N), to study the changes in the H due to solar flares. ΔH is obtained by subtracting the average midnight value of H to avoid the Earth's main field effect on the H component. The X-ray flux data recorded by the Geostationary Operational Environmental Satellite (GOES) satellites is obtained from the USA National Oceanic and Atmospheric Administration (http://www.sec.noaa.gov). The Local time (LT)=Universal Time (UT)+5.5 h. In the present study we have estimated the change in amplitude ΔA as, $\Delta A = A_{perturb} - A_{normal}$, where $A_{perturb}$ is the maximum VLF amplitude observed during the given solar flare event and A_{normal} is the mean amplitude for five normal days close to the flare event. The time difference between amplitude peak and X-ray flux peak Δt as $\Delta t = t_{Amax} - t_{FF}$ where t_{Amax} is the amplitude peak time of VLF signal and t_{FF} is flare flux peak time. Similarly, the change in ΔH due to flare is estimated as using $\Delta H_S = \Delta H_{Perturb} - \Delta H_{Normal}$ where $\Delta H_{Perturb}$ is the maximum change in ΔH observed during solar flare event and ΔH_{Normal} is the average for three international quiet days close to the flare event.

3. Observations

3.1. Solar flare effect on NWC signal at low latitude station: Allahabad

After the long solar minima, the Sun unleashed the first C-class flare of solar cycle 24 on 19 January 2010 at 14:17 LT, the strongest solar flare detected in almost two years. During January 2010–February 2011, nearly 41 solar flare events (21 C-class, 19 M-class

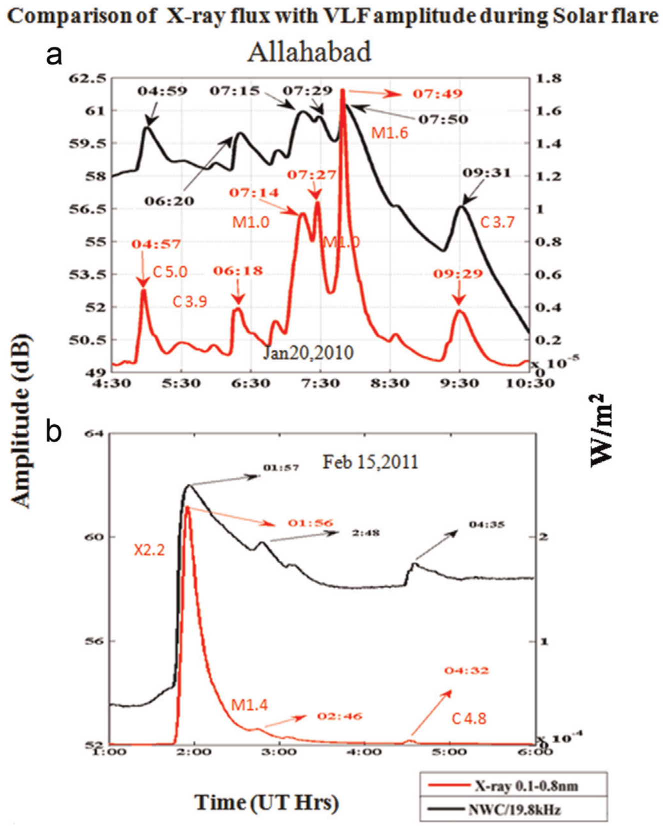

Fig. 2. An example of variation of X-ray flux (red line) detected by GOES and NWC VLF signal amplitude (black line) at Allahabad station on 20th January and 15th February 2011.

and 01 X-class flares) have been analyzed to examine the changes in VLF amplitude, Wait parameters, electron density and local time dependence of flares effect.

Fig. 2(a and b) shows an example of the amplitude perturbations in the NWC VLF signal received at Allahabad corresponding to the X-ray flux (GOES data) for 20th January 2010 and 15th February 2011 solar flares, respectively. The amplitude enhancements are observed for 3 C and 3 M-class flares that occurred on 20 January 2010. And also on 15th February 2011 for one C, one M and one X-class flares. These enhancements are due to extra D-region ionization. The extra ionization sharpens the D-region or upper boundary of the EIWG and lowers it up to several kilometres depending on the intensity of solar flare flux (Thomson and Clilverd, 2001; Grubor et al., 2005). When VLF signal propagates through the region of enhanced electron concentration, it finds a sharper boundary which gives a mirror type of reflection (Grubor et al., 2005) as a result the amplitude of the VLF signals is increased.

Table 1 gives the details of all the solar flare events considered in the present study. The change in the VLF signal amplitude (ΔA) depends on the flare strength (solar X-ray flux) which can be effectively utilized to estimate the electron density changes due to solar flares (Grubor et al., 2005; Zigman et al., 2007). Fig. 3 shows variation in the ΔA of NWC signal with solar flare intensity measured in dB relative to 1 $\mu W/m^2$ for all 41 solar flares. It can be seen that ΔA varies between 1.21 to 2.73 dB for C class solar flares and between 2.88 to 5.45 dB for M class solar flares. The lowest flare which produced the perturbation in the signal amplitude is a C 2.0 class flare (1.21 dB).The maximum ΔA of 6.8 dB was observed for an X2.2 solar flare. The solar flare X-ray flux intensities are expressed in decibel (dB) unit. A third-degree polynomial is used to fit the data points as its best fit. McRae and Thomson (2004) estimated the best-fit curve for the amplitude perturbation *versus* flare power, which can be used to determine the flare of higher classes (> X17) when GOES detector saturates. In general, as the intensity of the flare increases, the ΔA also increases but not linearly. For example, the ΔA for three C-class flares, C5.0, C3.9 and C3.7 occurred on 20th January 2010, were estimated 2.73 dB, 2.46 dB and 1.44 dB, respectively. However some inconsistency in the ΔA values were seen when solar flares of same class/strength occurred on different days. For example, C5.2 flare on 19th January 2010 (at 14:37 LT) produced $\Delta A \sim 1.68$ dB which is less as compared to C3.9 class flare on 20th January 2010 (11:50 LT) with $\Delta A \sim 2.46$ dB. The nonlinearity comes from the fact that ΔA also depends upon pre-flare flux condition and local time. In order to check it we have made a detailed analysis of the pre-flare X-ray flux for all the 41 flare events. A window of 15 min for solar X-ray flux is taken for all the solar flares before the onset and the average flux in this window is calculated (pre-flare level). This average flux is then subtracted from the peak flux value to obtain absolute enhancement in the flux level. The pre-flare flux conditions give better results when multiple solar flares occur in a short time. Based upon calculations, in general, it is observed that the pre-flare flux values follow the linear trend with the class of flares. But the preflux values show discrepancy when a flare is followed by another flare depending upon its class, *i.e.,* if the given flare is preceded by a higher class flare, the preflux value is more but the absolute enhancement in the flux is less. For example, on 15th February 2011, three successive flares occurred in the morning period (X 2.2, M1.4 and C4.8). The absolute flux enhancement is highest ($\sim 2.29 \times 10^{-4}$ W/m^2) for X2.2 flare among all the flares considered in the study. For M1.4 flare which was followed by X2.2, the flux level was stable as seen from Fig. 2, so the preflux level for M1.4 flare is more ($\sim 9.63 \times 10^{-5}$ W/m^2) as compared to that of X 2.2 (9.07×10^{-7} W/m^2). For C4.8 class flare the preflux level came nearly to the normal value ($\sim 2.14 \times 10^{-6}$ W/m^2). Similarly, C5.2 flare on 19th January 2010 had a preflux of $\sim 3.95 \times 10^{-7}$ W/m^2 which is less as compared to C3.9 flare with pre-flux of $\sim 2.15 \times 10^{-6}$ W/m^2 due to the fact that the later flare was followed by C5.0 flare.

The other reason for the nonlinearity is the local time dependence of solar flare effect. The local daytime taken into consideration is the daytime at the receiving station, Allahabad, between 06–18 LT (00:30–12:30 UT). In order to clearly understand local time dependence of ΔA and other D-region parameters, whole local daytime is divided in three periods: morning (06–10 LT), noon (10–15 LT) and evening (15–18 LT). Table 2 presents the average values of ΔA, Δt, H' and β for C and M-class flares. From Table 2, it can be seen that the average ΔA for C-class flares increases as the day progresses and attains its maximum value at noon and then decreases in the evening period. For M-class flares, the average value of ΔA during noon is less than that in the morning and evening periods. This is because of the occurrence of high intensity M-class flares in the morning (M6.4 at 08:06 LT) and evening period (M6.0 at 15:45 LT) as compared to noon, which results in higher ΔA ($\sim$5.45 dB and 5.2 dB, respectively). Fig. 4a shows the dependence of ΔA on the local time. As we have only one X-class flare event during the period of the present study, it is not possible to study local time dependence for X-class solar flare effects. Thomson and Clilverd (2001) studied solar flare effects both on long (12,000 km) and short (617 km) VLF propagation paths and showed that ΔA variation is less pronounced for long path as compared to the short path. Our present work shows that ΔA variation due to flares depends on the class of flares, preflare condition and local time.

Solar flare effect also shows time delay (Δt) in the occurrence of the VLF peak amplitude when compared to the time of X-ray

Table 1
Values of H' and β for different classes of flares calculated for VLF signal observed at Allahabad from the NWC transmitter signal using LWPC V 2.1. The other parameters such as change in the amplitude (ΔA), delay time are also shown.

Solar flare day	UT (h)	LT (h)	Flare class	ΔA (dB)	H' (km)	β (km^{-1})	Delay time (Δt) (min)	ΔH $H(nT)$
20100119	08:47	14:17	C 5.2	1.70	72.0	0.35	2	
	09:07	14:37	C 5.2	1.68	72.2	0.36	1	
20100120	04:59	10:29	C 5.0	2.73	69.9	0.38	2	
	06:20	11:50	C 3.9	2.46	70.5	0.37	2	
	07:15	12:45	M1.0	3.02	68.0	0.39	1	
	07:29	12:59	M1.0	3.05	68.5	0.39	2	
	07:50	13:20	M1.6	3.26	67.5	0.41	1	
	09:31	15:01	C3.7	1.44	76.0	0.28	2	
20100206	05:40	11:10	M1.3	3.15	68.0	0.40	1	
	07:09	12:39	C4.0	1.48	73.0	0.34	2	03.57
20100207	02:36	08:06	M6.4	5.45	66.0	0.40	2	
	04:54	10:24	M1.0	2.98	68.8	0.38	1	05.36
20100208	07:44	13:14	M4.0	3.52	66.0	0.42	1	10.30
	08:46	14:16	C2.8	1.52	73.2	0.33	2	
20100209	01:28	06:58	C3.0	1.56	76.1	0.30	3	
	04:20	09:50	C3.0	1.49	73.4	0.32	2	
20100212	07:28	12:58	C8.0	2.48	70.5	0.37	2	06.17
20100612	01:01	06:31	M2.0	3.11	71.0	0.35	2	
	09:20	15:50	C6.0	2.24	72.4	0.33	2	01.20
	11:12	16:42	M2.0	3.35	67.0	0.37	2	
20100613	05:42	11:12	M1.0	3.01	68.1	0.39	1	08.52
20110128	01:05	06:35	M1.4	3.06	70.8	0.36	2	
20110209	01:34	07:04	M1.9	3.09	70.4	0.37	2	
20110214	08:01	13:31	C3.0	1.32	73.4	0.32	2	02.50
	08:49	14:19	C6.0	2.07	71.0	0.37	2	
20110215	01:57	07:27	X2.2	6.80	64.0	0.42	1	04.20
	02:48	08:18	M1.4	3.01	71.1	0.39	2	
	04:32	10:02	C4.8	1.88	72.1	0.36	3	
20110216	01:06	06:36	C2.0	1.21	76.6	0.27	3	
	01:44	07:14	M1.0	2.99	71.0	0.39	2	
	05:52	11:22	C6.0	2.10	71.0	0.37	2	04.50
	06:28	11:58	C3.0	1.45	73.5	0.33	2	
	07:46	13:16	M1.0	3.05	71.0	0.39	1	
	09:15	14:45	M1.1	2.93	71.8	0.33	2	
	10:34	16:04	C3.0	1.27	76.7	0.27	3	
20110218	04:55	10:25	C4.0	1.54	73.1	0.33	2	05.40
	06:36	12:06	M1.0	2.88	69.5	0.39	1	
	07:27	12:57	C8.0	2.54	70.4	0.37	2	05.83
	09:16	14:46	C4.2	1.60	76.0	0.30	2	
	10:15	15:45	M6.0	5.20	66.0	0.39	2	
20110224	07:35	13:05	M3.5	3.94	67.0	0.38	2	13.00

flux peak. For example, on 20th January 2010, six peaks in the VLF amplitude were matched with the peaks in GOES X-ray flux data (Fig. 2a and b). The peaks of the C-class flare flux data occurred at 4:57 UT, 6:18 UT and 9:29 UT and the corresponding peaks in the VLF amplitude occurred at 4:59 UT, 6:20 UT and 9:31 UT, respectively. For M-class flares the X-ray flux peaks occurred at 7:14 UT, 7:27 UT and 7:49 UT and the corresponding peaks in the VLF amplitude occurred at 7:15 UT, 7:29 UT and 7:50 UT. From the above example, it can be seen that Δt is different for different classes of flares and it may also depend on the local time at the receiving station at the time of occurrence of solar flare. In order to examine this, we have plotted Δt *versus* local time for C, M and X-class flares in Fig. 4(b). Fig. 4b shows that, Δt for all flares, varies from $\sim$1–3 min, which is different for different classes of flares and also varies according to their occurrence time. In general, Δt is minimum for higher class (X) and maximum for lower class (C) flares. For C-class flares, Δt varies between $\sim$1–3 min which is higher in the morning and evening periods and lower in the noon period as seen from Table 2. For M-class flares, Δt is $\sim$2 min in the morning and evening periods and $\sim$1 min in the noon period. For X class flare, Δt is approximately 1 min. The Δt observed in the present work has been discussed by many workers with different terminology such as 'sluggishness' (Appleton, 1953; Valnicek and Ranzinger, 1972) and 'relaxation time' (Mitra, 1974). But the detailed study on the dependence of Δt on the class of flares was not examined. The Δt is caused by the D-region recombination–ionization processes to recover balance under the increased X-ray irradiance of the flare (Zigman et al., 2007). The Δt for all solar flares are given in Table 1. The Δt varies between $\sim$1–3 min and is consistent with previous observations (Mitra, 1974; Zigman et al., 2007; Grubor et al., 2005, Kumar and Kumar, 2014).

Mitra (1974) established a relationship between Δt and maximum electron density and showed that Δt is inversely related to the electron density, which is lower for higher electron density, *i.e.*, ionospheric response is faster when electron density is high. Hence, for the X-class flare the D-region response is fastest, resulting in minimum Δt value. Valnicek and Ranzinger (1972) using the X-ray data obtained by Inter-Cosmos 1 satellite, showed that 'sluggishness' (Δt) decreases when solar induced ionization increases and *vice versa*. Grubor et al. (2005) studied the VLF response to solar flares for short (~2000 km) path and showed that the Δt also depends on the solar zenith angle. The results presented here for medium ($\sim$6000 km) path length (Clilverd et al., 2001) at the Indian low latitude station show significant variation in Δt due to solar flares depending upon their classes and time of occurrence.

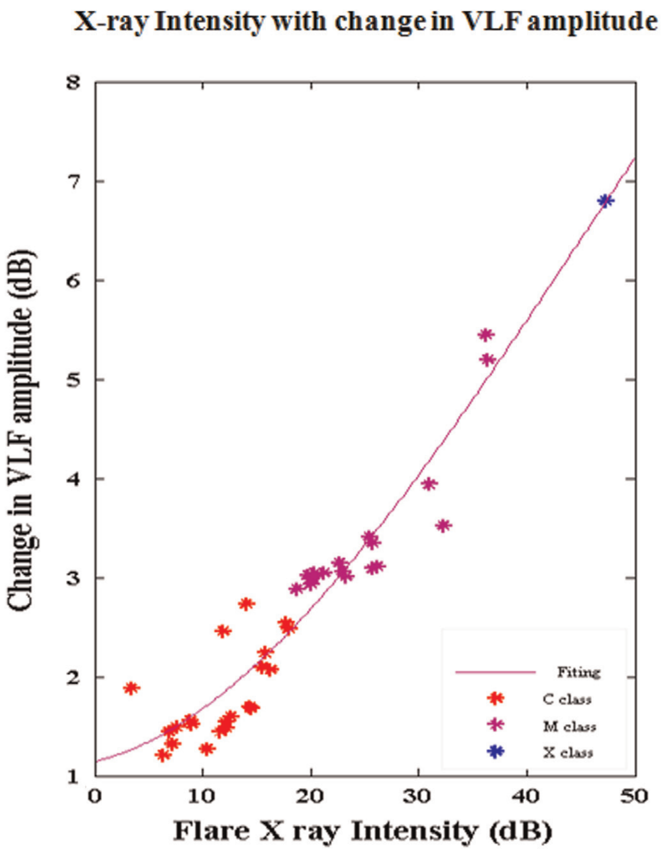

Fig. 3. Variation of change in the VLF amplitude with the solar flare intensity (dB).

Table 2
Average values of ΔA, Δt, H' and β during three different time periods (morning, noon, evening) for C and M class flares.

Time period	Delay time (Δt) (min)	ΔA (dB)	β (km^{-1})	H' (km)
C class				
Morning (6–10 LT)	2.67	1.42	0.30	75.37
Noon (10–15 LT)	2.00	1.92	0.35	72.14
Evening (15–18 LT)	2.50	1.36	0.28	76.35
M class				
Morning (6–10 LT)	2.00	3.45	0.38	70.05
Noon (10–15 LT)	1.27	3.16	0.39	68.56
Evening (15–18 LT)	2.00	4.28	0.38	66.50

3.2. Solar flare effect on Earth's magnetic field H component at the equatorial station: Tirunelveli

The variation in the horizontal component (H) of the Earth's magnetic field observed at Tirunelveli, an equatorial station (Geographic lat. 0.03°N, long. 150.40°E, dip latitude: 0.4°N), Indian sector, for solar flares (January 2010–February 2011), is examined and the change in ΔH (ΔH_s) due to flares is quantitatively studied. The geomagnetic activity is also examined during flare events to identify any effect of geomagnetic storms on the (ΔH). Chakrabarty et al. (2013) extensively investigated the moderate and low intensity solar flares effects on equatorial electrojet current. The transient electric field disturbances can occur during storm sudden commencement (SSC) and prompt penetration electric field associated with sub storms (Chakrabarty et al., 2010), which can mask the signatures caused by low and moderate solar flares in ΔH (Chakrabarty et al., 2013). The observations considered in this work are carefully investigated for the effects of transient field due to SSC and sub storms by looking in to the IEFy along with AL and Sym-H (Chakrabarty et al., 2013). After careful investigation, the possibility of any influence of transient electric field disturbances, during solar flares, associated with the current study cannot be completely ruled out. It was found that 12 out of 41 flare events (07 C-class, 04 M-class and 01 X-class) have shown changes in the ΔH. For example, the variations in ΔH for the flares of 6th February 2010, 15th and 24th February 2011, are shown in Fig. 5. The ΔH values on flare day (red line) and averaged on 3 international quiet days (black line) are plotted for three hour durations with respect to flare occurrence time in order to find the change in the ΔH due to solar flares. The C4.0 solar flare on 6th February 2010 had start, peak and end times at 12:30 LT, 12:39 LT and 12:44 LT, respectively. The corresponding response times in ΔH were identified at 12:31 LT, 12:40 LT and 12:45 LT, respectively. The M3.5 solar flare on 24th February 2011 started at 12:53 LT, with maximum flux at 13:05 LT and ended at 13:12 LT. The corresponding response in ΔH is observed at 12:57 LT, 13:07 LT and 13:17 LT, respectively. Similarly, for the X2.2 solar flare on15th February 2011 starting at 7:14 LT with its peak at 7:26 LT and ending at 7:36 LT, the corresponding response times in the ΔH was observed at 7:20 LT, 7:28 LT and 7:39 LT, respectively. Moderate increase of ~3.57 nT and ~4.2 nT in ΔH given by ΔH_s is seen during the solar flares on 06 February 2010 and 15 February 2011 for C4.0 and X2.2, respectively. On 24 February 2011, a significant increase in ΔH of ~13 nT is observed for M3.5 class flare which occurred at 13:07 LT. Similarly, from Table 1, significant increase in ΔH is observed for the flare events in the noon time when equatorial electrojet (EEJ) strength is maximum at the equatorial stations. Rastogi et al. (1999) observed positive impulse (increase) in the ΔH at equatorial and near equatorial stations. Fig. 6 shows the local time dependence of ΔH for 12 selected flare events that have shown change in ΔH. It is clear from Fig. 6 that only those flare events which occurred during noon period have shown the significant change in ΔH except for X class flares which occurred in the morning period (~07:27 LT) and produced the significant increase in ΔH giving ΔH_s of 4.2 nT.

4. Estimation of wait D-region parameters: LWPC modeling

In order to quantify the solar flare induced perturbations in the D-region ionosphere, we have utilized the Long Wavelength Propagation Capability (LWPC) code v 2.1 developed by US Navy (Ferguson, 1998). This code is used to calculate the changes in the Wait ionospheric parameters (Wait and Spies, 1964), ionospheric reflection height (H') and exponential sharpness factor (β), due to solar flares.

Fig. 7 shows the normal day (unperturbed) diurnal variation of the NWC signal (amplitude and phase averaged for 5 days) received at Allahabad (blue line) matched with the LWPC modeled VLF amplitude (red line). The VLF amplitude and phase have been modeled for three different time periods of a local day (as discussed in Section 3.1): 00:30–4:30 UT (06:00–10:00 LT) near the morning terminator (morning period), 09:30–12:30 UT (15:00–18:00 LT) near evening terminator (evening period) and the third one is the period between morning and evening terminators 04:30–9:30 UT (10:00–15:00 LT) (noon period) during which the VLF amplitude is almost stable. In order to match the observed VLF amplitude and phase of NWC signal on the normal day with the VLF amplitude estimated by LWPC, the values of amplitude and phase of NWC signals recorded with the AWESOME receiver were added 35 dB and 15°, respectively, to calibrate it. After the calibration the model was run for every 15 min from 0 UT to 12 UT to account for the temporal changes in the signal amplitude and phase. The H' and β were chosen for the best matching between

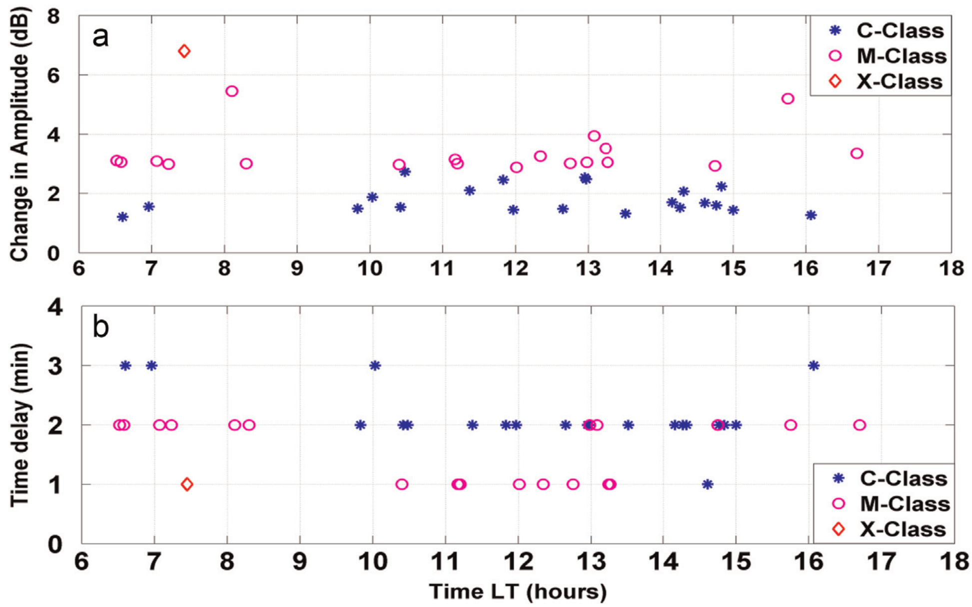

Fig. 4. (a) Local time variation of change in the VLF NWC signal amplitude estimated with respect to normal day for C, M and X-classes of flare. (b) Local time variation of time delay for C, M and X-classes of flares.

the LWPC amplitude and phase and the recorded amplitude and phase. The values of H' and β parameters were found almost the same for both morning and evening periods. The average values of H' and β for unperturbed (normal) daytime ionosphere, were estimated as (a) β=0.26 km^{-1} and H'=77 km for the interval near terminators (morning and evening periods) and (b) β=0.30 km^{-1} and H'=74 km for the noon period. The noon time values of H' and β for the normal day match well with previous studies (McRae and Thomson, 2004; Thomson et al., 2005; Grubor et al., 2005, 2008; Zigman et al., 2007) for low and mid latitude regions.

During solar flares, the amplitude of the sub-ionospheric VLF wave enhances and the corresponding phase advances. The perturbation in the VLF amplitude during solar flare is also modeled using LWPC in the same way as for the normal day. In order to match the estimated values using model with the observed values, the LWPC code was run for every 5 min and the output values were noted. Fig. 8 shows the modeling plot of the amplitude and phase of NWC signals for the solar flare on 20th January 2010. The H' and β values estimated by using LWPC for solar flares considered in the present study are given in Table 1.

5. Results and discussion

5.1. Variation in wait D-region ionospheric parameters due to solar flares

During solar flares, the increased ionization results in descent of upper edge of EIWG which is shown by decrease in H' and increase in β values (Grubor et al., 2008). Table 1 shows the H' and β values estimated using LWPC model for all solar flares considered in the present study. For C-class solar flares on 20th January 2010, the average change in H' and β values were estimated 3 km and 0.06 km^{-1}, respectively, whereas for M-class flares these values are 6 km and 0.10 km^{-1}, respectively, with respect to the normal daytime values. The strongest solar flare of class-X on 15th February 2011 (which occurred in the morning period) showed highest decrease in H' by 13 km and increase in β by 0.16 km^{-1}, with respect to the unperturbed day time values. This indicates that H' and β are different for different classes of flares and also they vary with local time *i.e.*, the solar zenith angle. The variation of H' and β with local time for C, M and X classes of flares is shown in Fig. 9a and b. In Fig. 9a, it is seen that H' is minimum for X-class flare and maximum for C class flares. From Table 2 it is seen that average H' value is maximum in the morning and evening periods and minimum in the noon period. The H' varies from 69.9 to 76.6 km for C-class flares. The H' for the M-class flares shows a similar trend. Table 2 shows that β follows an opposite trend as compared to H'. The β is maximum for X-class flare and minimum for C-class flares. The average value of β for C-class flare shows that β is minimum in the morning and evening periods and maximum in the noon period. The β varies from 0.27 to 0.42 km^{-1} for C-class flares. The β for the M-class flares shows similar trend. The maximum and minimum changes in H' and β are estimated to be 13 km, 0.16 km^{-1} for X2.2 flare and 0.4 km, 0. 01 km^{-1} for C2.0 flare, respectively.

McRae and Thomson (2004) showed that solar flares reduce the H', which is proportional to the logarithm of X-ray flux intensity. They found that the H' reduced down to 58 km from its normal unperturbed day value of 71 km and β significantly increased and reached a saturation value of about 0.52 km^{-1} for extremely intense flares of magnitude greater than about X17. Thomson and Clilverd (2001) estimated the H' and β to be 64.6 km and 0.485 km^{-1}, respectively, for M2.4 class flare as compared to normal values of H'=71 km and β=0.43 km^{-1}. Zigman et al. (2007) observed a decrease in H' to 69 km and an increase in β to about 0.54 km^{-1} from normal values of H'=74 km and β=0.30 km^{-1} for NAA (24.0 kHz) transmitter signal amplitude received at Belgrade. Our estimations of Wait parameters (H' and β) are in agreement with previous studies as discussed above.

5.2. Enhancement in D-region electron density due to solar flares

The normal day time D-region ionosphere is maintained by the Solar Lyman-α (121.5 nm) radiation which ionizes minor constituent nitric oxide and forms the main source of ionization. It has been known that cosmic rays also cause a significant proportion of ionization in the D-region ionosphere (Rishbeth and Garriott,

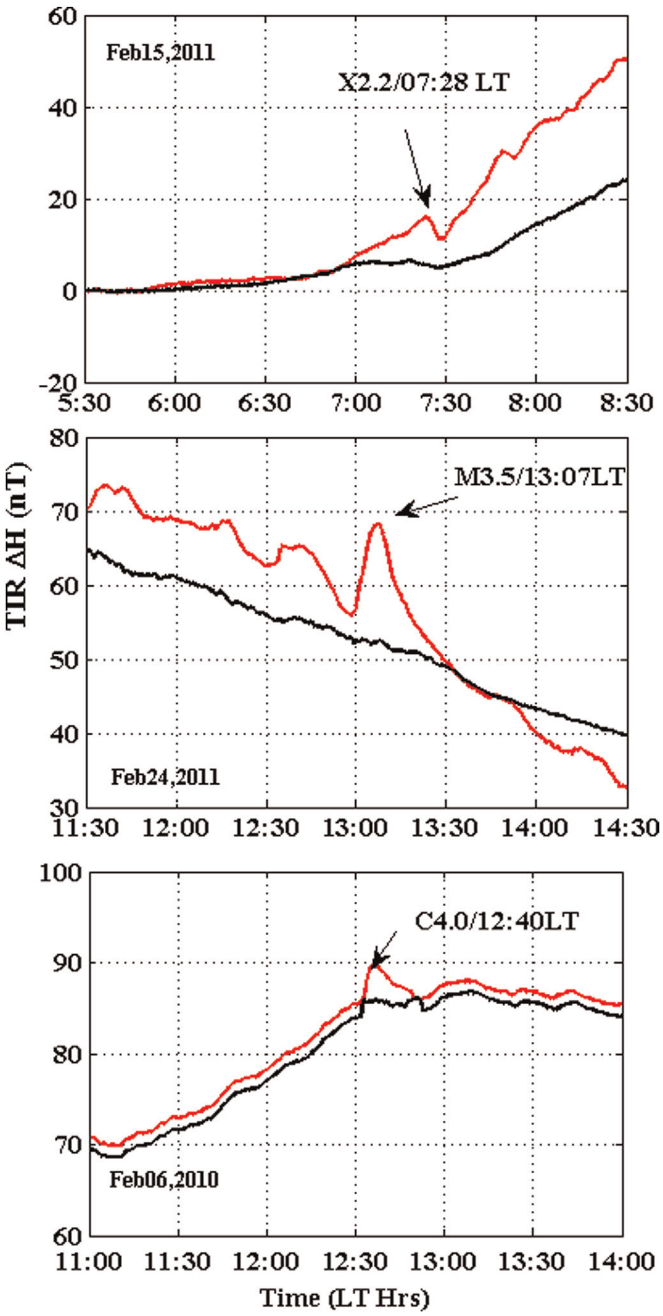

Fig. 5. Variation in the Earth's magnetic field horizontal component (H) obtained using one second magnetic data from the Indian equatorial station Tirunelveli (Geographic lat., 8.7°N, long., 77.8°E, dip lat., 0.4°N) for solar flare events of C, M and X-classes.

1969). During solar flares the X-ray flux from the solar flare becomes the dominant source of ionization and overcomes ionization caused by galactic cosmic rays and the Lyman-α radiation, thereby significantly increasing the ionization which causes decrease in the H' and increase in the β (Grubor et al., 2008). The electron density profile can be estimated by using Eq. (1) given as (Wait and Spies, 1964).

$$N_e(z) = 1.43 \times 10^7 \exp(-0.15H') \exp[(\beta - 0.15)(z - H')] \quad (1)$$

where $N_e(z)$ is the electron density in cm^{-3}. The electron density profile obtained by this method is valid up to 100 km altitude. We have estimated the increase in electron density in the height range of 60–80 km, using Wait parameters (H' and β) obtained from the LWPC modeling of solar flare perturbed amplitude and phase of NWC signal at Allahabad. Fig. 10 represents the electron density profile obtained from modeled H' and β values for the flares that occurred on 20th January 2010, 9th and 15th February 2011 in the (a) noon and (b) morning and evening periods and their comparison with normal day profile (green line). The strongest flare recorded in the present study (X2.2) showed a maximum enhancement in electron density when compared to all other solar flares. The VLF amplitude response to the flare induced increase in the electron density is almost instantaneous, behaving as a monotonic function of the electron density (Zigman et al., 2007).

The extra ionization due to flares not only increases the electron density at the reflection height but also changes it along height of the D-region (Thomson and Clilverd, 2001). The change in the electron density is computed by taking difference of electron density during flare event and during the normal day at reference height of 70 km. and presented in Table 1. The C-class flares on 20th January 2010 and one on 15th February 2011 perturbed the daytime D-region ionosphere by increasing the electron density by ~20 times with respect to the normal day time values. The two M-class flares observed on 20th January 2010 and one each on 9th and 24th February 2011 increased electron density by ~41 times as compared to normal day values. The X-class flare observed on 15th February 2011 showed the highest change in the electron density which is ~80 times over the normal day value. The electron density profile strongly depends on β (Thomson and Clilverd, 2001; McRae and Thomson, 2004) and hence on the change in the VLF amplitude. For a C-class flare the change in the electron density ranges from a minimum of 5 el/cc to a maximum of 220 el/cc at the estimated reference height of 70 km. Kolarski and Grubor (2009) for M-class flares, estimated increase in the electron density of the order of two for the GQD and NAA transmitter signals received at Belgrade, Serbia. Our results from an Indian low latitude station are almost consistent with previous observations in other parts of the world (Zigman et al., 2007, Grubor et al., 2005). Fig. 11 shows the change in the electron density with flare X-ray flux in dB. The change in electron density is minimum for the C-class flares and maximum for X2.2 flare. The

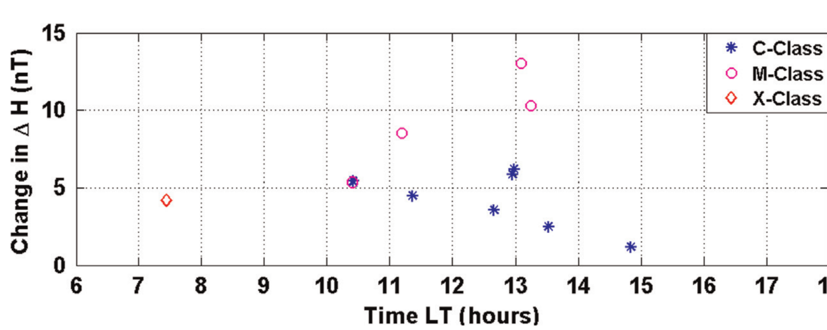

Fig. 6. Local time variation in the changes in the horizontal component (ΔH) of geomagnetic field for C, M and X-classes of flares.

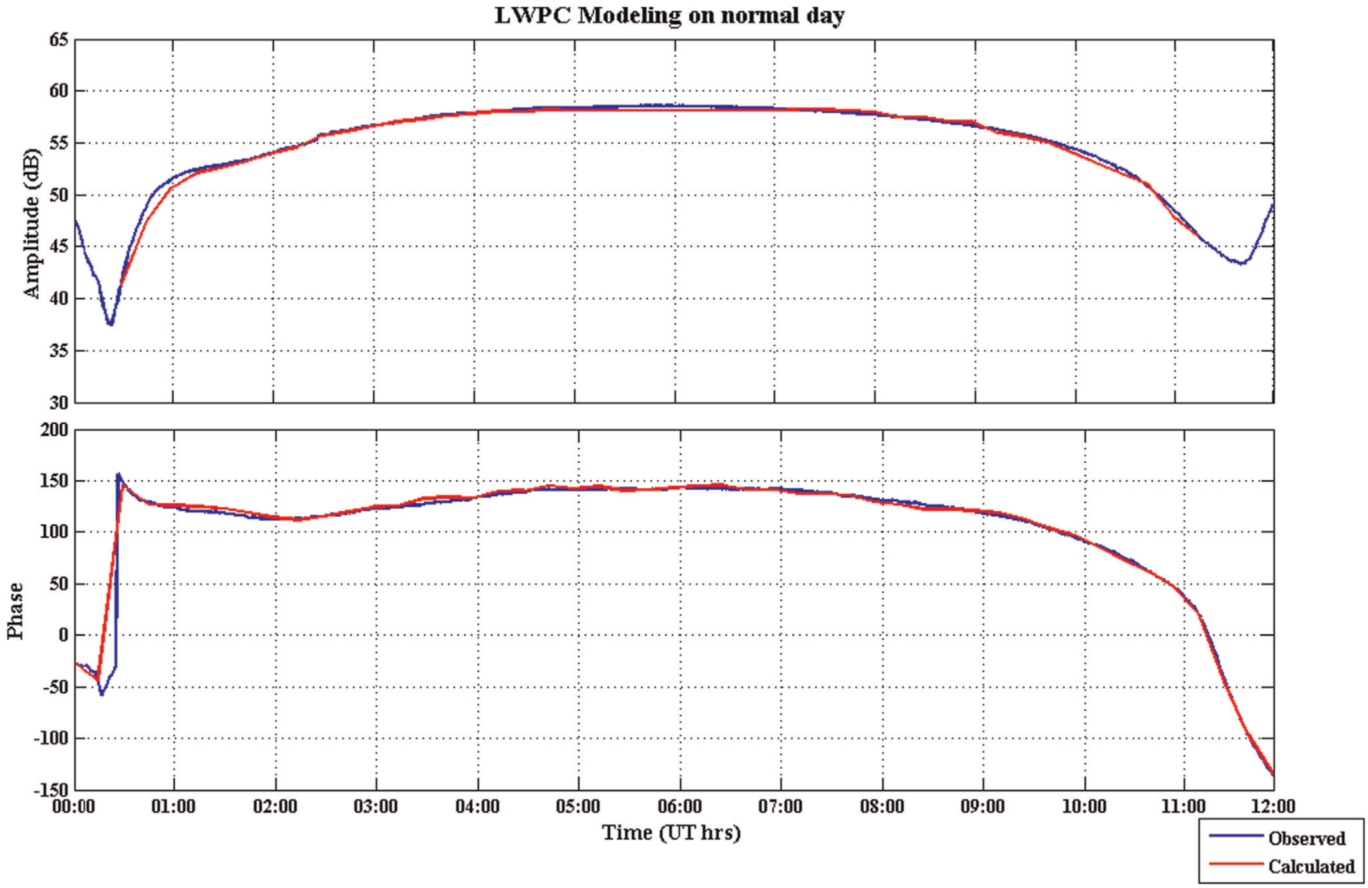

Fig. 7. An example of normal day time amplitude (upper panel) and phase (lower panel) variation of NWC signal (19.8 kHz) at Allahabad, India (blue line). The modeled variation using LWPC is shown by a red line.

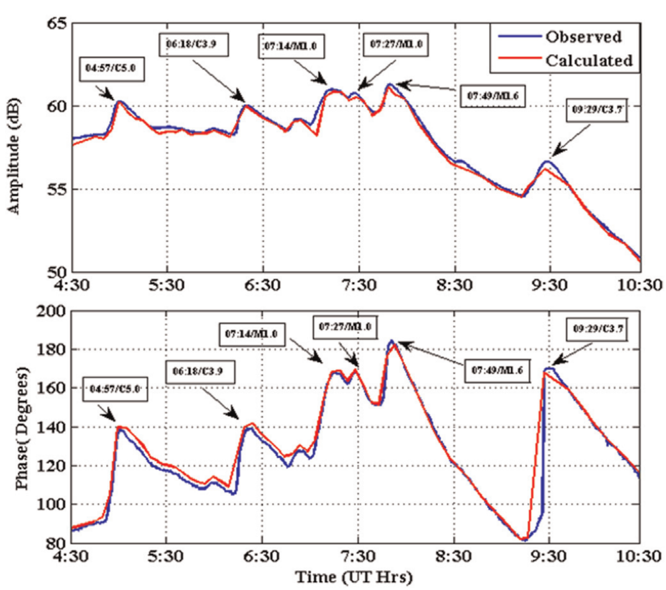

Fig. 8. Modeled VLF amplitude and phase for 20 January 2010 solar flare using LWPC code v 2.1.

best-fit lines (pink) show that electron density increases with increase in solar flux intensity. There are few events where C-class flares have produced more electron density changes compared to M-class flares. This can be attributed to local time variation of solar flare effect and pre-flare D-region condition and X-ray flux (Han and Cummer, 2010; Ohya et al., 2011; Maurya et al., 2012a,b; Maurya et al., 2014a,b).

5.3. Effect of solar flare on Earth's magnetic field at the equatorial station: Tirunelveli

As mentioned in Section 3.2, the solar flare events of C, M, X classes produced moderate increase in the H-component of Earth's geomagnetic filed (indicated by ΔH, Fig. 5) at an Indian equatorial station, Tirunelveli. The solar flare of the M 3.5 class on 24th February 2011 produced a significant increase of about 13 nT in the ΔH given by ΔH_s. Some of the earlier works show that the solar flares can decrease the H component of Earth's magnetic field at the electrojet stations and outside the electrojet region (Sastri, 1975). Based on the study of several solar flare events over Indo-Russian region, Rastogi et al., (1999) found that during normal equatorial electrojet (EEJ) events, solar flares show a positive increase in H component at all stations. Rastogi et al. (1999) studied the changes in the H component (ΔH) in response with solar flares at different latitudes. The ΔH during solar flare follows the latitude which is similar to solar quiet Sq (Rastogi et al., 1999) variation. The change in EEJ system corresponding to the solar flare has been studied by Manju et al. (2009). Solar flares increase the ΔH during electrojet events and decrease the ΔH during the counter electrojet times (Manju and Viswanathan, 2005) similar to our observations. The local time dependence of solar flare effect shows that effect is more pronounced in the noon period for C and M class flares. This non linearity in ΔH can be attributed to the local time variation of E region zonal electric field in the equatorial region (Chakrabarty et al., 2013). The absence of background changes in E-region ionization with the local time may result in the linear change in ΔH with respect to the flare intensity. Recently, Sripathi et al. (2013) for X7/2B flare on 09th August 2011

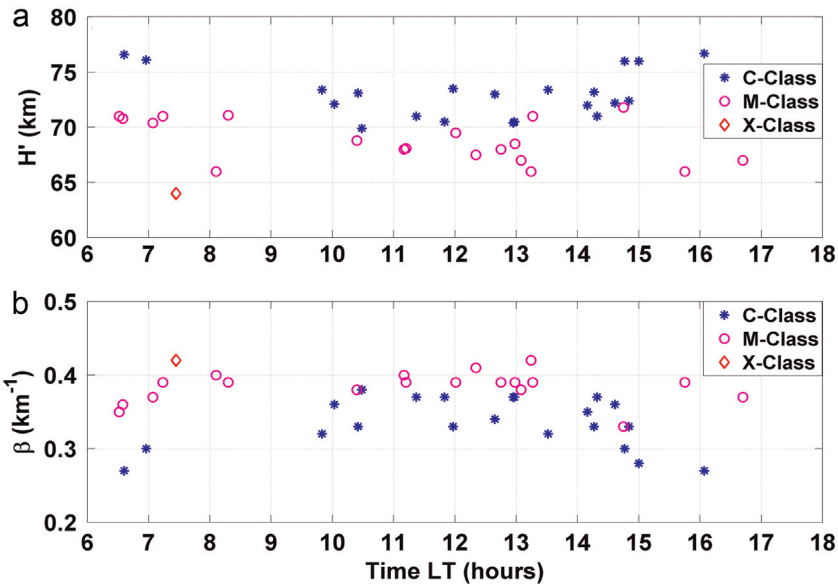

Fig. 9. (a) Local time variation of reflection height (H') with respect to normal day for C, M and X classes of flares. (b) Local time variation of sharpness factor (β) for C, M and X classes of flares.

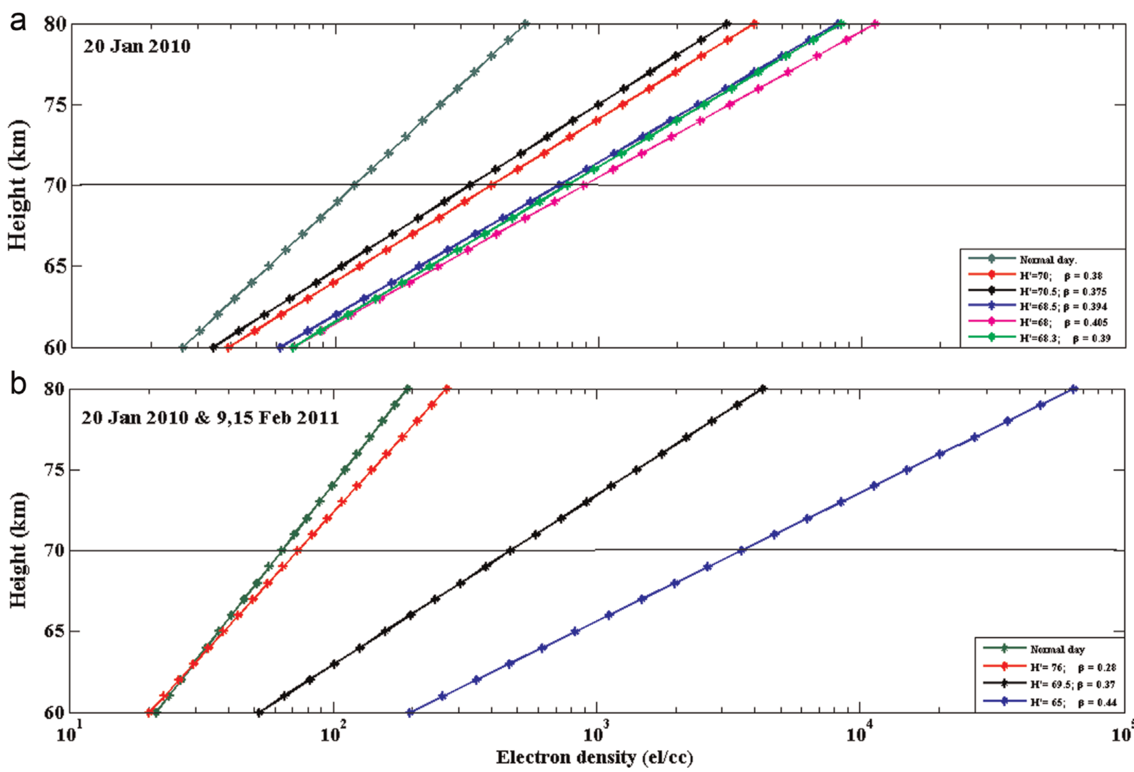

Fig.10. (a) Comparison of electron density profiles for flares on 20th January 2010 in the noon period (10–15 LT h) and on normal day at Allahabad. (b) Comparison of the electron density profile for solar flares on 20th January 2010 and 9th and 15th February 2011 in the morning and evening periods (06–10 LT h and 15–18 LT h) with the normal day for Allahabad. (Horizontal line at 70 km is added as reference height for comparison of electron density).

with peak flux at 08:05 UT (13:35 LT h) observed a decrease in H at Tirunelveli and suggested that it is due to change in E-region electron density and the strong ionospheric currents due to presence of counter electrojet during the flare occurrence time. However, we have not observed any decrease in ΔH for the solar flare events considered in the present study.

6. Summary

Solar flare effects on the sub-ionospheric VLF signals are identified by the sudden increase in their amplitudes and advancement in the phases. These sudden changes are manifestations of rapid enhancements in the D-region ionospheric plasma

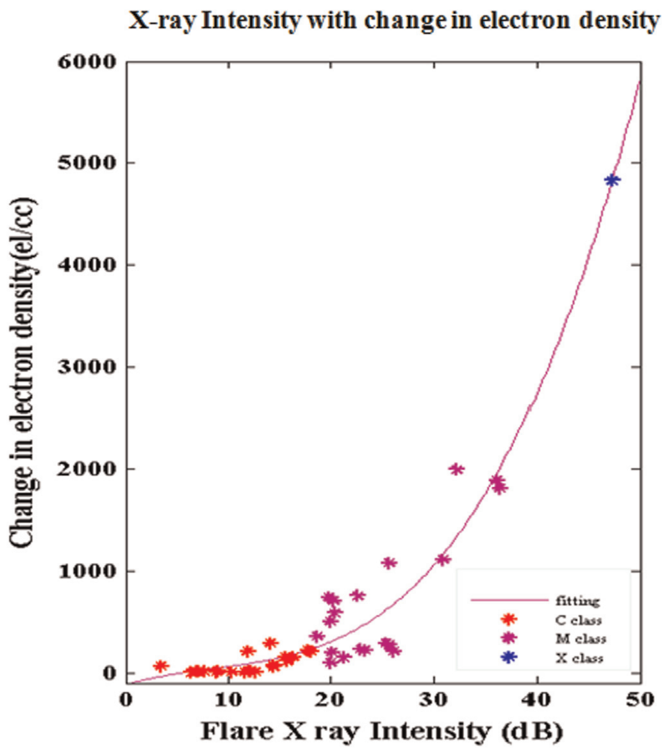

Fig. 11. Comparison of electron density at 70 km with the solar flare intensity (dB).

density associated with flares. We have analyzed the effect of C, M and X-class solar flares on NWC signal (19.8 kHz) recorded at Allahabad, a low latitude station in the Indian region, during the period of one year from January 2010 to February 2011. Also the solar flare effect on the horizontal component of the Earth's magnetic field (H) at the Indian equatorial station, has been examined. The period of study falls under low solar activity of the current solar cycle 24. It is found that change in the VLF amplitude (ΔA), time delay (Δt) between VLF peak amplitude and X-ray flux peak and D-region ionospheric parameters (H' and β) strongly depend on the intensity (class) of flares, pre-flare condition and local time of flare occurrence. This dependence has been tested for C, M and X-class of flares during morning, noon and evening periods of local day time (06–18 LT). The results show that ΔA varies between 1.21–6.8 dB for C to X-class of flares. The Δt varies from 1–3 min for different classes of flares and is minimum for X class of flare. The local time dependence for ΔA and Δt indicates an opposite trend with ΔA increasing as the day progresses and attaining its maximum value at noon and then decreasing until evening. The maximum increase of $\sim$7 dB in the NWC signal amplitude was observed for X 2.2 solar flare event on 15th February 2011. The LWPC modeling code has been utilized to estimate the changes in the reflection height H' and sharpness factor β for all the solar flare events. Reduction in the H' and increase in the β are estimated during the flares as compared to the normal day time values. The maximum change in the H' and β is estimated for X-class flare followed by M-class and C-class flares which is consistent with earlier studies (Zigman et al., 2007; Grubor et al., 2008). The local time dependence of changes in H' and β indicates an opposite trend and change is maximum during the noon period. The electron density profiles estimated during the solar flare events show a maximum increase in electron density of the order of $\sim$80 times as compared to the normal day values for X- class flare at the reference altitude of 70 km. The increase of about $\sim$13 nT in ΔH for solar flare of M-class was observed at Tirunelveli which could be accounted for the enhanced electrojet during the solar flares. The investigation is in progress for high solar activity of the current solar cycle which will provide us further opportunity to study the D-region and geomagnetic field response to solar flares with larger dataset.

Acknowledgments

Authors from the Indian Institute of Geomagnetism (IIG) are grateful to the Director, IIG, for support and encouragement to carry out the project and work. Authors from IIG also thank India–Japan Science Cooperative Program project DST/INT/JSPS/P-137/2012. All authors also thank the International Space Weather Initiative Program (ISWI) and the United Nations Basic Space Sciences Initiative (UNBSSI) program for their support of VLF project activities in India and Fiji. Thanks to CAWSES India, Phase-II program for the financial support to carry out VLF research activities (grant no: E33015/7/20/2010-V). AKM thanks to CSIR, India for financial support in the form of research associateship (grant no: 9/1123(0001)/2K14-485 EMR-I) .

References

Ananthakrishnan, S., Abdu, M.A., Piazza, L.R., 1973. D-region recombination coefficients and the short wavelengths X-ray flux during a solar flare. Planet. Space Sci. 21, 367–375.

Appleton, E.V., 1953. A note on the "sluggishness" of the ionosphere. J. Atmos and Terr. Phys. 3 (5), 282–284.

Bainbridge, G., Inan, U.S., 2003. Ionospheric D-region electron density profiles derived from the measured interference pattern of VLF waveguide modes. Radio Sci. 38 (4), 1077–1098. http://dx.doi.org/10.1029/2002RS002686.

Chakrabarty, D., Sekar, R., Sastri, J.H., Pathan, B.M., Reeves, G.D., Yumoto, K., Kikuchi, T., 2010. Evidence for OI 630.0 nm day glow variations over low latitudes during onset of a substorm. J. Geophys. Res 115, A10316. http://dx.doi.org/10.1029/2010JA015643.

Chakrabarty, D., Mala Bagiya, S., Smitha thampi, V., Pathan, B.M., Sekar, R., 2013. Signatures of moderate (M-class) and low (C and B class) intensity solar flares on the equatorial electrojet current: case studies. J. Atmos. Solar Terr. Phys. 105–106 (2013), 170–180.

Clilverd, M.A., Rodger, C.J., Thomson, N.R., Lichtenberger, J., Steinbach, P., Cannon, P., Angling, M.J., 2001. Total solar eclipse effects on VLF signals: observation and modeling. Radio Sci. 36 (4), 773–788.

Davies, K., 1990. Ionospheric Radio, Electromagnetic Wave Series 31 Peregrines. London.

Ferguson, J.A., 1998. Computer Programs for Assessment of Long-Wavelength Radio Communications. Space and Naval Warfare Systems Center, San Diego, CA (Version 2.0).

Grubor, D.P., Šulic´, D.M., Zigman, V., 2008. Classification of X-ray solar flares regarding their effects on the lower ionosphere electron density profile. Ann. Geophys. 26, 1731–1740.

Grubor, D., Sulic, D., Zigman, V., 2005. Influence of solar X-ray flares on the earth ionosphere wave guide. Serb. Astron. 171, 29–35.

Han, F., Cummer, S.A., 2010. Midlatitude daytime D region ionosphere variations measured from radio atmospherics. J. Geophys. Res. 115, A10314. http://dx.doi.org/10.1029/2010JA015715.

Hargreaves, J.K., 2003. The Solar-Terrestrial Environment. Cambridge University Press, New York.

Kolarski, A., Grubor, D., 2009. Study of the X-Ray Flare Induced Lower Ionosphere Changes by Simultaneous Monitoring of Two VLF Signals: GQD and NAA.In: Proceedings of the URSI.

Kumar, A., Kumar, S., 2014. Space weather effects on the lowlatitude D-region ionosphere during solar minimum. Earth Planets Space 66 76-1:76-10.

Manju, G., Viswanathan, K.S., 2005. Response of the equatorial electrojet to solar flare related X-ray flux enhancements. Earth Planets Space 57, 231–242.

Manju, G., Pant, T.K., Devasia, C.V., Ravindran, S., Sridharan, R., 2009. Electrodynamical response of the Indian low-mid latitude ionosphere to the very large solar flare of 28 October 2003 – a case study. Ann. Geophys. 27, 3853–3860.

Maurya, A.K., Singh, R., Veenadhari, B., Pant, P., Singh, A.K., 2010. Application of lightning discharge generated radio atmospherics/tweeks in lower ionospheric plasma diagnostics. J. Phys.: Conf. Ser. 208, http://dx.doi.org/10.1088/1742-6596/208/1/012061 012061-1012061-7.

Maurya, A.K., Singh, R., Veenadhari, B., Cohen, M.B., Kumar, S., Selvakumaran, R., Pant, P., Singh, A.K., Inan, U.S., 2012a. Morphological features of tweeks and nighttime D region ionosphere at tweek reflection height from the observations in the low-latitude Indian sector. J. Geophys. Res. 117, A05301. http://dx.doi.org/10.1029/2011JA016976.

Maurya, A.K., Veenadhari, B., Singh, R., Kumar, S., Cohen, M.B., Selvakumaran, R., Gokani, S., Pant, P., Singh, A.K., Inan, U.S., 2012b. Nighttime D region electron density measurements from ELF-VLF tweek radio atmospherics recorded at low latitudes. J. Geophys. Res. 117, A11308. http://dx.doi.org/10.1029/2012JA017876.

Maurya, A.K., Singh, R., Kumar, S. Kumar, D.V., Veenadhari, B., 2014a. Waves-like signatures in the D-region ionosphere generated by solar flares. In: Proceedings of the IEEE General Assembly and Scientific Symposium (URSI GASS), XXXIth URSI. 10.1109/URSIGASS.2014.6929796.

Maurya, A.K., Phanikumar, D.V., Singh, R., Kumar, S., Veenadhari, B., Kwak, Y.-S., Kumar, A., Singh, A.K., Kumar., K.N., 2014b. Low-mid latitude D region ionospheric perturbations associated with 22 July 2009 total solar eclipse: wave-like signatures inferred from VLF observations. J. Geophys. Res., 8512–8523. http://dx.doi.org/10.1002/2013JA019521.

McRae, W.M., Thomson, N.R., 2000. VLF phase and amplitude: daytime ionospheric parameters. J. Atmos. Solar Terr. Phys. 62, 609–618.

McRae, W.M., Thomson, N.R., 2004. Solar flare induced ionospheric D-region enhancement from VLF phase and amplitude observations. J. Atmos. Solar Terr. Phys. 66, 77–87.

Mitra, A.P., 1974. Ionospheric Effects of Solar Flares. D. Reidel Publishing Company, Dordrecht-Holland.

Morfitt, D.G., Shellman, C.H., 1976. MODESRCH, an improved computer program for obtaining ELF/VLF/LF mode constants in an Earth-ionosphere waveguide. Nav. Electron. Lab. Cent., Interim Rep., 77T; .

Ohya, H., Shiokawa, K., Miyoshi, Y., 2011. Long-term variations in tweek reflection height in the D and lower E-regions of the ionosphere. J. Geophys. Res. 116, A10322. http://dx.doi.org/10.1029/2011JA016800.

Pant, P., 1993. Relation between VLF phase deviations and solar X-ray fluxes during solar flares. Astrophys. Space Sci. 209, 297–306.

Phanikumar, D.V., Kwak, Y.-S., Patra, A.K., Maurya, A.K., Singh, R., Park, S.M., 2014. Response of the mid-latitude D-region ionosphere to the total solar eclipse of 22 July 2009 studied using VLF signals from South Korean peninsula. Adv. Space Res. 54 (6), 961–968. http://dx.doi.org/10.1016/j.asr.2014.06.005.

Rastogi, R.G., Pathan, B.M., Rao, D.R.K., Sastry, T.S., Sastri, J.H., 1999. Solar flare effects on the geomagnetic elements during normal and counter electrojet periods. Earth Planets Space 51, 947–957.

Rishbeth, H., Garriott, O.K., 1969. Introduction to Ionospheric Physics. Academic Press, New York, London.

Sastri, J.H., 1975. The geomagnetic solar flare effect of 6 July 1968 and its implications. Ann. Geophys. 31, 481–485.

Singh, A.K., Singh, R., Veenadhari, B., Singh, A.K., 2012. Response of low latitude D-region ionosphere to the total solar eclipse of 22 July 2009 deduced from ELF/VLF analysis. Adv. Space Res. 50, 1352–1361. http://dx.doi.org/10.1016/j.asr.2012.07.005.

Singh, A.K., Singh, A.K., Singh, R., Singh, R.P., 2013. Solar flare induced D-region ionospheric perturbations evaluated from VLF measurements. Astrophys. Space Sci., 1–9. http://dx.doi.org/10.1007/s10509-013-1699-4.

Singh, R., Veenadhari, B., Cohen, M.B., Pant, P., Singh, A.K., Maurya, A.K., Vohat, P., Inan, U.S., 2010. Initial results from AWESOME VLF receivers: set up in low latitude Indian regions under IHY2007/UNBSSI. Curr. Sci. 98 (3), 398–405.

Singh, R., Veenadhari, Maurya, A.K., Cohen, M.B., Kumar, S., Selvakumaran, R., Pant, P., Singh, A.K., Inan, U.S., 2011. D-region ionosphere response to the Total Solar Eclipse of 22 July 2009 deduced from ELF-VLF tweek observations in the Indian sector. J. Geophys. Research 116, http://dx.doi.org/10.1029/2011JA016641, A10301:1-9.

Sripathi, S., Balachandran, N., Veenadhari, B., Singh, R., Emperumal, K., 2013. Response of the equatorial and low latitude ionosphere to an intense X-class solar flare (X7/2B) as observed on 09 August 2011. J. Geophys. Res. 118, 2648–2659. http://dx.doi.org/10.1002/jgra.50267.

Thomson, N.R., McRae, W.M., 2009. Nighttime ionospheric D region: equatorial and nonequatorial. J. Geophys. Res. 114, A08305. http://dx.doi.org/10.1029/2008JA014001.

Thomson, N.R., Clilverd, M.A., 2001. Solar flare induced ionospheric D-region enhancements from VLF amplitude observations. J. Atmos. Solar Terr. Phys. 63 (7), 1729–1737.

Thomson, N.R., Clilverd, M.A., McRae, W.M., 2007. Nighttime D region parameters from VLF amplitude and Phase. J. Geopys. Res. 112, A07304. http://dx.doi.org/10.1029/2007JA91227.

Thomson, N.R., Rodger, C.J., Dowden, R.L., 2004. Ionosphere gives size of greatest solar flare. Geophys. Res. Lett. 31, L06803. http://dx.doi.org/10.1029/2003GL019345.

Thomson, N.R., Rodger, C.J., Clilverd, M.A., 2005. Large solar flares and their ionosperic D region enhancements. J. Geophys. Res. 110, A06306. http://dx.doi.org/10.1029/2005JA011008.

Tsurutani, B.T., Verkhoglyadova, O.P., Mannucci, A.J., Lakhina, G.S., Li, G., Zank, G.P., 2009. A brief review of “solar flare effects” on the ionosphere. Radio Sci. 44, RS0A17. http://dx.doi.org/10.1029/2008RS004029.

Valnicek, B., Ranzinger, P., 1972. X-ray emission and D-region ‘sluggishness’. Bull. Astron. Inst. Czechoslov 23, 318–322.

Wait, J.R., Spies, K.P., 1964. Characteristics of the earth ionosphere wave guide for VLF radio waves. National Bureau of Standards, NBS technical noteU.S. Government printing office, 300; .

Zigman, V., Grubor, D., Suli´c, D., 2007. D-region electron density evaluated from VLF amplitude Δt during X-ray solar flares. J. Atmos. Solar Terr. Phys. 69 (7), 775–792.